

# Suppression of phase separation and giant enhancement of superconducting transition temperature in $\text{FeSe}_{1-x}\text{Te}_x$ thin films

Yoshinori Imai \*, Yuichi Sawada \*, Fuyuki Nabeshima \*, and Atsutaka Maeda \*

\*Department of Basic Science, the University of Tokyo, Tokyo, Japan

Submitted to Proceedings of the National Academy of Sciences of the United States of America

**We demonstrate the successful fabrication on  $\text{CaF}_2$  substrates of  $\text{FeSe}_{1-x}\text{Te}_x$  films with  $0 \leq x \leq 1$ , including the region of  $0.1 \leq x \leq 0.4$ , which is well known to be the “phase-separation region”, via pulsed laser deposition which is a thermodynamically non-equilibrium method. In the resulting films, we observe a giant enhancement of the superconducting transition temperature,  $T_c$ , in the region of  $0.1 \leq x \leq 0.4$ : the maximum value reaches 23 K, which is approximately 1.5 times as large as the values reported for bulk samples of  $\text{FeSe}_{1-x}\text{Te}_x$ . We present a complete phase diagram of  $\text{FeSe}_{1-x}\text{Te}_x$  films. Surprisingly, a sudden suppression of  $T_c$  is observed at  $0.1 < x < 0.2$ , while  $T_c$  increases with decreasing  $x$  for  $0.2 \leq x < 1$ . Namely, there is a clear difference between superconductivity realized in  $x = 0 - 0.1$  and in  $x \geq 0.2$ . To obtain a film of  $\text{FeSe}_{1-x}\text{Te}_x$  with high  $T_c$ , the controls of the Te content  $x$  and the in-plane lattice strain are found to be key factors.**

$\text{FeSe}_{1-x}\text{Te}_x$  | thin film growth | compressive strain | complete phase diagram

Abbreviations: PLD, pulsed laser deposition; XRD, X-ray diffraction

Since the discovery of superconductivity in  $\text{LaFeAs}(\text{O},\text{F})$ [1], many studies concerning iron-based superconductors have been conducted.  $\text{FeSe}$  is the iron-based superconductor with the simplest crystal structure[2]. The  $T_c$  of  $\text{FeSe}$  is approximately 8 K, which is not very high in comparison with other iron-based superconductors. However, the value of  $T_c$  strongly depends on the applied pressure, and the temperature at which the resistivity becomes zero,  $T_c^{\text{zero}}$ , reaches as high as  $\sim 30$  K at 6 GPa[3]. This suggests that  $\text{FeSe}$  samples with higher  $T_c$  are available by the fabrication of thin films because we can introduce lattice strain. Indeed, we have previously reported that  $\text{FeSe}$  films fabricated on  $\text{CaF}_2$  substrates exhibit  $T_c$  values approximately 1.5 times higher than those of bulk samples because of in-plane compressive strain[4]. On the other hand, superconductivity with  $T_c$  of 65 K has recently been reported in a monolayer  $\text{FeSe}$  film on  $\text{SrTiO}_3$ [5, 6]. It is unclear whether this superconductivity results from the characteristics of the interface. However, this finding indicates that  $\text{FeSe}$  demonstrates potential as a very-high- $T_c$  superconductor.

The partial substitution of Te for Se in  $\text{FeSe}$  also raises  $T_c$  to a maximum of 14 K at  $x = 0.5 - 0.6$ [7]. In  $\text{FeSe}_{1-x}\text{Te}_x$ , it is well known that we cannot obtain single-phase samples with  $0.1 < x < 0.4$  because of phase separation[7]. Here, we focus on this region of phase separation. Generally, the process of film deposition involves crystal growth in a thermodynamically non-equilibrium state. Thus, film deposition provides an avenue for the synthesis of a material with a metastable phase. In this letter, we report the fabrication of epitaxial thin films of  $\text{FeSe}_{1-x}\text{Te}_x$  with  $0 \leq x \leq 1$  on  $\text{CaF}_2$  substrates using the pulsed laser deposition (PLD) method. We demonstrate that single-phase epitaxial films of  $\text{FeSe}_{1-x}\text{Te}_x$  with  $0.1 \leq x \leq 0.4$  are successfully obtained and that the maximum value of  $T_c$  is as large as 23 K, which is higher than the previously-reported values for bulk and film samples of  $\text{FeSe}_{1-x}\text{Te}_x$ [7, 8, 9, 10, 11, 12], except for those of the mono-

layer  $\text{FeSe}$  films[5, 6]. Our results clearly show that the optimal Te content for the highest  $T_c$  for  $\text{FeSe}_{1-x}\text{Te}_x$  films on  $\text{CaF}_2$  is different from the widely-believed value for this system.

Figure 1a presents the X-ray diffraction patterns of  $\text{FeSe}_{1-x}\text{Te}_x$  films for  $x = 0 - 0.5$  on  $\text{CaF}_2$ . Here and hereafter, the Te content  $x$  of our films represents the nominal Te composition of the polycrystalline target. With the exception of an unidentified peak in the  $\text{FeSe}_{0.5}\text{Te}_{0.5}$  film, only the 00 $l$  reflections of a tetragonal  $\text{PbO}$ -type structure are observed, which indicates that these films are well oriented along the  $c$  axis. Figures 1b and 1c present enlarged segments of these plots near the 001 and 003 reflections, respectively. The  $2\theta$  values of the peak positions decrease with increasing  $x$  in a continuous manner, which is consistent with the fact that the  $c$ -axis length increases with increasing  $x$ . It should be noted that the values of the full widths at half maximum (FWHM),  $\delta(2\theta)$ , of the  $\text{FeSe}_{1-x}\text{Te}_x$  films with  $x = 0.1 - 0.4$ , which is known as the region of phase separation in the bulk samples[7], are  $\delta(2\theta) = 0.2 - 0.3^\circ$  for the 001 reflection and  $\delta(2\theta) = 0.4 - 0.6^\circ$  for the 003 reflection, which are nearly the same as the values for the  $\text{FeSe}$  and  $\text{FeSe}_{0.5}\text{Te}_{0.5}$  films. This result is in sharp contrast to the previously-reported result that the FWHM was broad *only* in films of  $\text{FeSe}_{1-x}\text{Te}_x$  with  $x = 0.1$  and  $0.3$ ,[13] where phase separation has been believed to occur. The results presented in Figs. 1a-1c indicate the formation of a single phase in our  $\text{FeSe}_{1-x}\text{Te}_x$  films with  $x = 0.1 - 0.4$ .

In Figure 1d, the  $c$ -axis lengths of 29 films of  $\text{FeSe}_{1-x}\text{Te}_x$  are plotted as a function of  $x$ . The values of the  $c$ -axis lengths vary

## Significance

To clarify the mechanism of superconductivity in iron-based superconductors, it is crucial to investigate  $\text{FeSe}_{1-x}\text{Te}_x$ , which has the simplest crystal structure among them. There is, however, a serious obstacle to the understanding of its superconductivity; phase separation occurs in the region of  $0.1 \leq x \leq 0.4$ , and thus a whole phase diagram has not been available. Here we report the successful fabrication of  $\text{FeSe}_{1-x}\text{Te}_x$  films with  $0 \leq x \leq 1$ . This is the first demonstration of the suppression of the phase separation. What is more notable is that a giant enhancement of  $T_c$  is observed in the “phase-separation region”. The complete phase diagram that we present provides a novel perspective for the mechanism of superconductivity of this material.

Reserved for Publication Footnotes

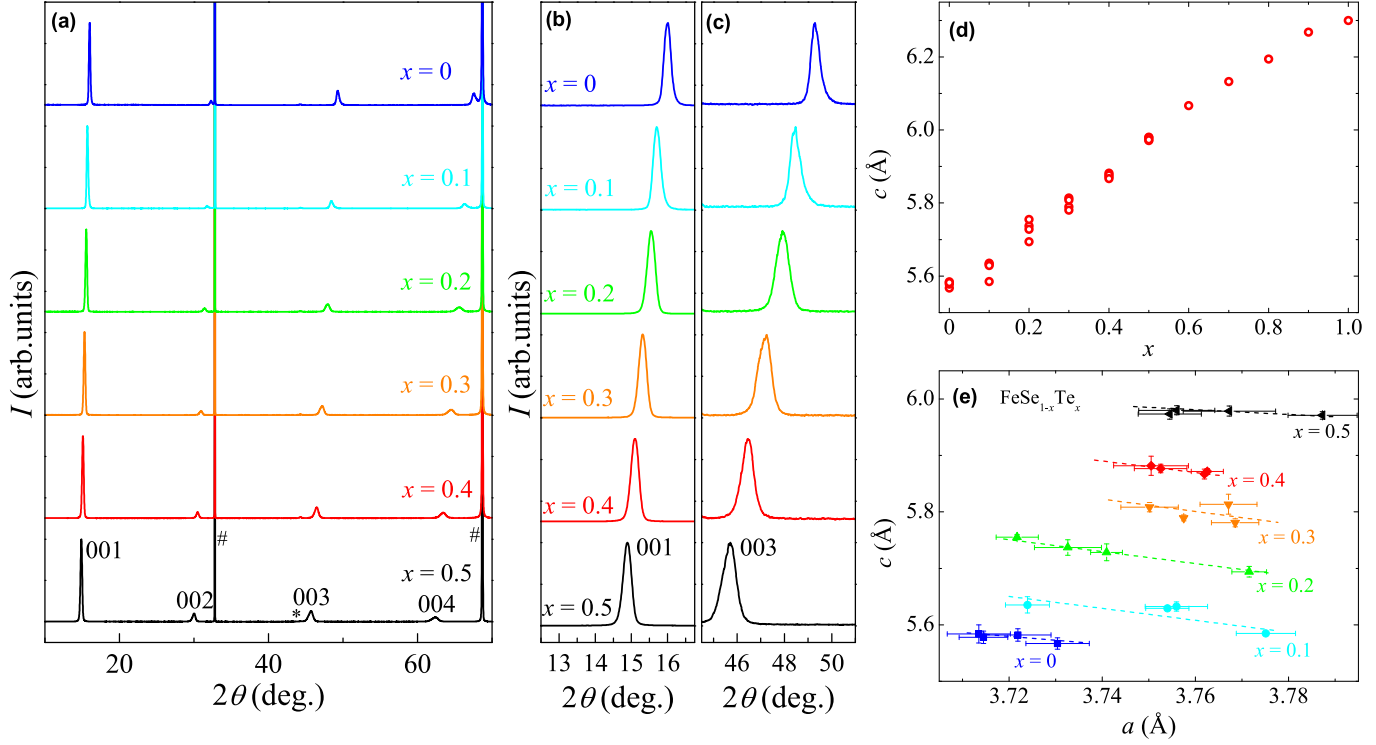


**Fig. 1.** (a) Out-of-plane X-ray diffraction patterns of  $\text{FeSe}_{1-x}\text{Te}_x$  thin films for  $x = 0 - 0.5$  with film thicknesses of 120-147 nm. The number signs represent peaks associated with the substrate. The asterisk represents an unidentified peak. Enlarged segments of the plots presented in (a) near the 001 and 003 peaks are shown in (b) and (c), respectively. (d) The  $c$ -axis lengths of  $\text{FeSe}_{1-x}\text{Te}_x$  films, where the  $x$  value indicated on the horizontal axis is the nominal Te content. (e) Relations between the  $a$ -axis and  $c$ -axis lengths in  $\text{FeSe}_{1-x}\text{Te}_x$  films. The colors and shapes of the symbols correspond to the Te content  $x$ , as shown in the figure. The dashed lines are guides for the eye. The data for  $x = 0$  and  $0.5$  presented in (a)-(e) are cited from our previous papers[4, 14].

almost linearly with the nominal Te contents of the targets in the whole range of  $x$  including both end-member materials. The evident formation of a single phase and the systematic change in the  $c$ -axis length strongly indicate that the nominal Te content of the polycrystalline target is nearly identical to that of the final  $\text{FeSe}_{1-x}\text{Te}_x$  film. Note that the compositional analysis of grown films using scanning electron microscopy/energy-dispersive X-ray (SEM/EDX) analysis is impossible for  $\text{FeSe}_{1-x}\text{Te}_x$  films on  $\text{CaF}_2$  substrates because the energies of the K-edge of Ca and the L-edge of Te are very close to each other. The above-mentioned features indicate that phase separation is suppressed in our  $\text{FeSe}_{1-x}\text{Te}_x$  films with  $x = 0.1 - 0.4$  on  $\text{CaF}_2$  substrates. To our knowledge, this result is the first manifestation of the suppression of phase separation in  $\text{FeSe}_{1-x}\text{Te}_x$  with  $x = 0.1 - 0.4$ .

Figure 1e presents the relations between the  $a$ -axis and  $c$ -axis lengths in films of  $\text{FeSe}_{1-x}\text{Te}_x$ . At first glance, there seems to be no relations between the  $a$ -axis length and  $x$ , in sharp contrast to the behavior of the  $c$ -axis length. The  $a$ -axis and  $c$ -axis lengths of films with the same  $x$  show a weak negative correlation. This behavior cannot be explained by a difference in Te content of a film, which should result in a positive correlation. By contrast, if variations in  $c$  are caused by a difference in in-plane lattice strain, this behavior can be explained in terms of the Poisson effect. Indeed, the  $a$ -axis lengths of films of  $\text{FeSe}$  and  $\text{FeSe}_{0.5}\text{Te}_{0.5}$  are smaller than those of bulk samples with the same composition. Thus, we consider that the  $a$ -axis length predominantly depends on the in-plane lattice strain rather than the Te content  $x$ . One might think that this behavior looks strange, because the lattice constant

of  $\text{CaF}_2$  ( $a_{\text{CaF}_2}/\sqrt{2}$ ) is longer than the  $a$  of  $\text{FeSe}_{1-x}\text{Te}_x$ , which usually leads to a tensile strain. In the previous paper, the penetration of  $\text{F}^-$  ions from the  $\text{CaF}_2$  substrates into the films has been proposed as a possible mechanism for nontrivial compressive strain in  $\text{FeSe}_{1-x}\text{Te}_x$  films on  $\text{CaF}_2$  substrates[15]. Because of smaller ionic radius of  $\text{F}^-$  than that of  $\text{Se}^{2-}$ , this peculiar compressive strain can be explained by the partial substitution of  $\text{F}^-$  for  $\text{Se}^{2-}$  near the interface between a film and a substrate.

Figures 2a-2d present the temperature dependences of the electrical resistivities,  $\rho$ , of 16 films of  $\text{FeSe}_{1-x}\text{Te}_x$  for  $x = 0.1 - 0.4$ . The value of  $T_c$  depends on the film thickness, even in films with the same  $x$ . The highest  $T_c^{\text{onset}}$ , which is defined as the temperature where the electrical resistivity deviates from the normal-state behavior, and the  $T_c^{\text{zero}}$  of the  $\text{FeSe}_{1-x}\text{Te}_x$  films are 13.2 K and 11.5 K, respectively, for  $x = 0.1$ ; 22.8 K and 20.5 K, respectively, for  $x = 0.2$ ; 20.9 K and 19.9 K, respectively, for  $x = 0.3$ ; and 20.9 K and 20.0 K, respectively, for  $x = 0.4$ . Compared with the results for bulk samples, a drastic enhancement of  $T_c$  is observed in these  $\text{FeSe}_{1-x}\text{Te}_x$  films. Surprisingly, the values of  $T_c^{\text{zero}}$  in the films with  $x = 0.2$  and  $0.4$  exceed 20 K. These values are larger than those reported for  $\text{FeSe}_{0.5}\text{Te}_{0.5}$  films[14, 8, 10, 11]. In particular, the  $T_c$  of the  $\text{FeSe}_{0.8}\text{Te}_{0.2}$  film with a thickness of 73 nm is approximately 1.5 times as high as those of bulk crystals of  $\text{FeSe}_{1-x}\text{Te}_x$  with the optimal composition,  $x \approx 0.5$ [7]. Based on the measurement of the  $\rho$  of the  $\text{FeSe}_{0.8}\text{Te}_{0.2}$  film under a magnetic field applied along the  $c$  axis, we estimate an upper critical field at 0 K of  $\mu_0 H_{c2} = 55.4$  T using the Werthamer-Helfand-Hohenberg(WHH) theory[16], which yields a Ginzburg-Landau coherence length at 0 K of

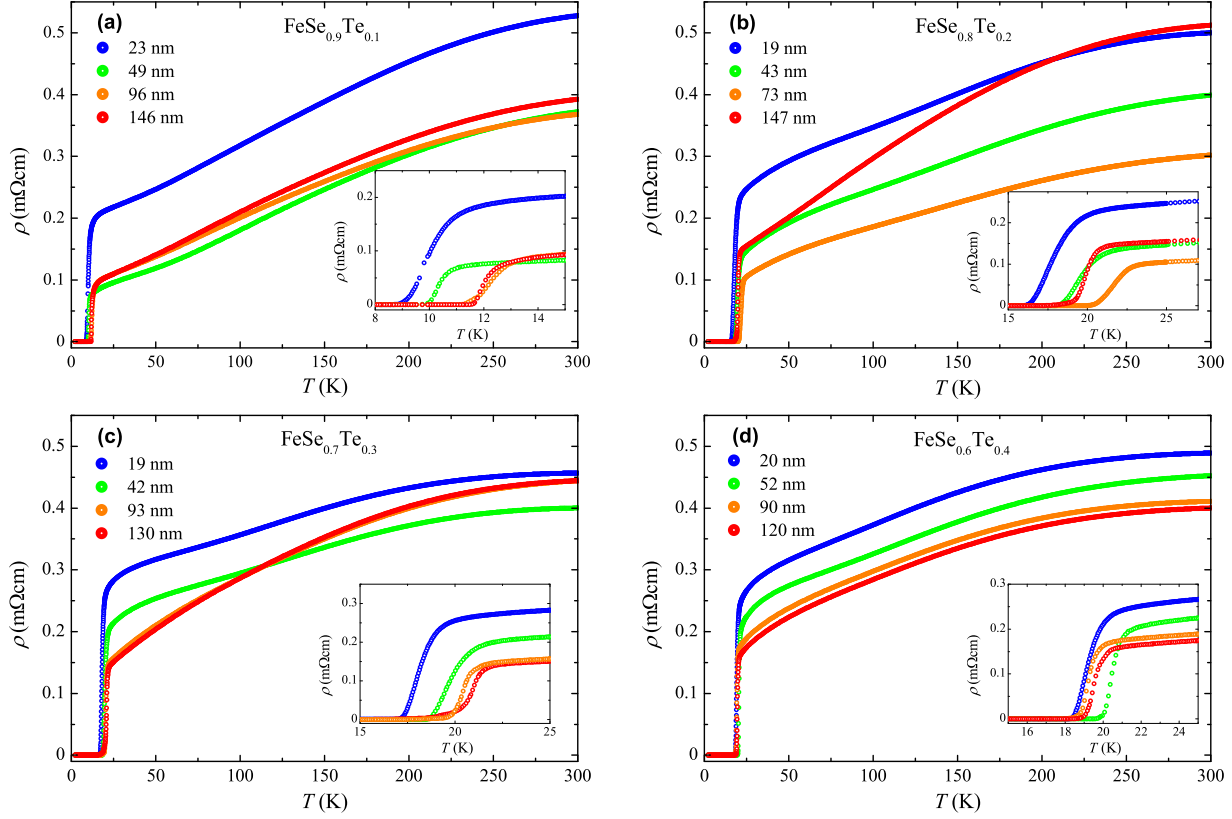


**Fig. 2.** Temperature dependences of the electrical resistivities,  $\rho$ , of FeSe<sub>1-x</sub>Te<sub>x</sub> thin films for (a)  $x = 0.1$ , (b)  $x = 0.2$ , (c)  $x = 0.3$  and (d)  $x = 0.4$  with different film thicknesses. The insets present enlarged views of the plots near the superconducting transition.

$\xi_{ab}(0) \sim 24.4$  Å (see the supporting information). This value of  $\mu_0 H_{c2}$  is approximately half the value for an FeSe<sub>0.5</sub>Te<sub>0.5</sub> film on CaF<sub>2</sub> with a  $T_c$  of approximately 16 K.[9]

Using the data shown above, we present the phase diagram of FeSe<sub>1-x</sub>Te<sub>x</sub> films on CaF<sub>2</sub> substrates in Fig. 3. For comparison, the data for bulk samples of FeSe<sub>1-x</sub>Te<sub>x</sub>[7, 17] are also plotted in this figure. In bulk crystals, the optimal Te content to achieve the highest  $T_c$  is considered to be  $x \approx 0.5$ , and phase separation occurs in the region of  $0.1 \leq x \leq 0.4$ [7]. However, our data clearly demonstrate that this phase separation is absent and that the optimal composition for an FeSe<sub>1-x</sub>Te<sub>x</sub> film on a CaF<sub>2</sub> substrate is not  $x \approx 0.5$  but  $x \approx 0.2$ . It should be noted that the dependence of  $T_c$  on  $x$  suddenly changes at the boundary defined by  $0.1 < x < 0.2$ . Unlike the “dome-shaped” phase diagram that is familiar in iron-based superconductors, the values of  $T_c$  in films with  $0.2 \leq x \leq 1$  increase with decreasing  $x$ , while the strong suppression of  $T_c$  is observed at  $0.1 < x < 0.2$ . The behavior in films with  $x \geq 0.2$  can be explained by the empirical law which shows the relation between  $T_c$  and structural parameters. In iron-based superconductors, it is well accepted that the bond angle of  $(Pn, Ch)\text{-Fe-(}Pn, Ch)$  ( $Pn = \text{Pnictogen}$ ,  $Ch = \text{Chalcogen}$ ),  $\alpha$ , [18, 19] and/or the anion height from the iron plane,  $h$ , [20] are the critical structural parameters that determine the value of  $T_c$ . In bulk samples of FeSe<sub>1-x</sub>Te<sub>x</sub>,  $\alpha$  and  $h$  approach their optimal values, i.e.  $\alpha = 109.47^\circ$  [18, 19] and  $h = 1.38$  Å [20], with decreasing  $x$  (down to  $x = 0$ ), which should be the same in FeSe<sub>1-x</sub>Te<sub>x</sub> films. Therefore, the increase of  $T_c$  in films with  $0.2 \leq x \leq 1$  with decreasing  $x$  can be explained by the optimization of  $\alpha$  and/or  $h$  based on the empirical law. However, the sudden suppression of  $T_c$  in films with  $0 \leq x < 0.2$  is not consistent

with this scenario, and its origin should be sought among other factors. We consider there are two candidates for this origin from the structural analysis of bulk samples of FeSe<sub>1-x</sub>Te<sub>x</sub>. One is the effect of the orthorhombic distortion. In a bulk sample of FeSe, a structural phase transition from tetragonal to orthorhombic occurs at 90 K [21]. However, in bulk samples of FeSe<sub>1-x</sub>Te<sub>x</sub> with  $x \sim 0.4 - 0.6$  which  $T_c$ s take optimum values, there are papers with different conclusions on the presence/absence of the similar type of the structural transition as that of FeSe [22, 23, 24]. It should be noted that a structural transition temperature is lower and that the orthorhombicity is much smaller than those of FeSe even in the report where the structural transition is present [24]. These results on crystal structures suggest that the orthorhombic distortion results in a suppression of  $T_c$ . This scenario is applicable to the behavior of our films, if a large orthorhombic distortion is observed only in films with  $x = 0 - 0.1$ . The other candidate is the change in the distance between the layers of Fe- $Ch$  tetrahedra,  $\delta$ . As shown in the supporting information, in polycrystalline samples of FeSe<sub>1-x</sub>Te<sub>x</sub>, the  $\delta$  value of FeSe is much smaller than those of FeSe<sub>1-x</sub>Te<sub>x</sub> with  $x \geq 0.5$  at which  $\delta$  is nearly independent of  $x$  [22]. We speculate that the decrease of  $\delta$  in FeSe is related with the suppression of  $T_c$ . Indeed, in polycrystalline samples, FeSe exhibits smaller values of  $\delta$  and  $T_c$  than does FeSe<sub>0.5</sub>Te<sub>0.5</sub> [7, 22], and the intercalation of alkali metals and alkaline earths into FeSe result in the  $c$ -axis length as large as approximately 20 Å and  $T_c$  as high as 45 K [25, 26]. At this moment, the origin of the suppression of  $T_c$  at  $0.1 < x < 0.2$  is unclear, which will be a subject of a future study. Regardless of its origin, we believe that it is reasonable to distinguish between superconductivity in  $x = 0 - 0.1$  and in  $x \geq 0.2$ . In other words, our phase diagram of Fig. 3 provides a new view

for superconductivity in  $\text{FeSe}_{1-x}\text{Te}_x$ , that is, a discontinuity in superconductivity of  $\text{FeSe}_{1-x}\text{Te}_x$ . We are able to come to this picture, only after the data for  $x = 0.1-0.4$  become available in this study. If we remove a cause for the suppression of  $T_c$  in  $x = 0, 0.1$  in some way, a further increase in  $T_c$  can be expected because of the optimization of structural parameters.

In conclusion, we prepared high-quality epitaxial thin films of  $\text{FeSe}_{1-x}\text{Te}_x$  on  $\text{CaF}_2$  substrates using the pulsed laser deposition method. We successfully obtained  $\text{FeSe}_{1-x}\text{Te}_x$  films with  $0.1 \leq x \leq 0.4$ , which has long considered to be the “phase-separation region”, using a thermodynamically non-equilibrium growth of film deposition. From the results of electrical resistivity measurements, a complete phase diagram is presented in this system, in which the maximum value of  $T_c$  is as high as 23 K at  $x = 0.2$ . Surprisingly, a sudden suppression of  $T_c$  is observed at  $0.1 < x < 0.2$ , while  $T_c$  increases with decreasing  $x$  for  $0.2 \leq x < 1$ . This behavior is different from the “dome-shaped” phase diagram that is familiar in iron-based superconductors.

### Materials and Methods

All of the  $\text{FeSe}_{1-x}\text{Te}_x$  ( $x = 0-1$ ) films in this study were grown by the pulsed laser deposition method using a KrF laser [27, 28]. Polycrystalline pellets with a nominal composition of  $\text{FeSe}_{1-x}\text{Te}_x$  ( $x = 0-1$ ) were used as the targets. The substrate temperature, repetition rate, and back pressure were 280 °C, 20 Hz, and  $10^{-7}$  Torr, respectively. Single crystals of the  $\text{CaF}_2$  (100), which is one of the most preferred materials for the thin-film growth of  $\text{FeSe}_{1-x}\text{Te}_x$  [9, 4], were used as the substrates. We used a metal mask to prepare the  $\text{FeSe}_{1-x}\text{Te}_x$  films in a six-terminal shape for transport measurements. The thicknesses of the thin films were measured using a Dektak 6 M stylus profiler and estimated to be 12-148 nm. The crystal structures and orientations of the films were characterized by four-circle X-ray diffraction (XRD) with  $\text{Cu K}\alpha$  radiation at room temperature. The  $a$ -axis and  $c$ -axis lengths are determined from the 204 and 00 $l$  reflections in XRD measurements, respectively. Electrical-

resistivity measurements were conducted using the four-terminal method from 2 K to 300 K with magnetic fields up to 9 T applied perpendicular to the film surface.

**ACKNOWLEDGMENTS.** We are grateful to Dr. Ichiro Tsukada at CRIEPI for fruitful discussions. The authors thank Profs. Jun-ichi Shimoyama and Kohji Kishio at Department of Applied Chemistry, the University of Tokyo for their especial support in the chemical-composition analysis of the films.

This work was partially supported by Strategic International Collaborative Research Program (SICORP), Japan Science and Technology Agency.

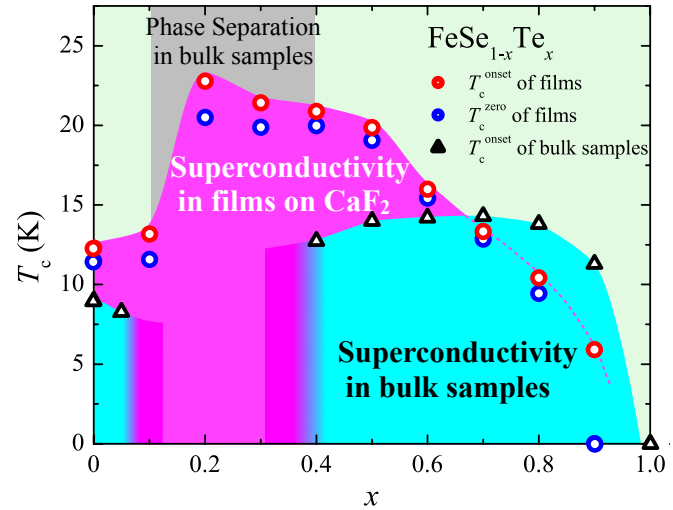


**Fig. 3.** Dependence of  $T_c$  on  $x$ . The red and blue circles represent the  $T_c^{\text{onset}}$  and  $T_c^{\text{zero}}$  values of the  $\text{FeSe}_{1-x}\text{Te}_x$  thin films, respectively. The black triangles represent the  $T_c^{\text{onset}}$  values obtained in measurements of the magnetic susceptibility of bulk samples [7, 17]. The dashed curve is a guide for the eye.

- Kamihara Y, Watanabe T, Hirano M, Hosono H (2008) Iron-based layered superconductor  $\text{La}[\text{O}_{1-x}\text{F}_x]\text{FeAs}$  ( $x = 0.050.12$ ) with  $T_c = 26$  K. *J. Am. Chem. Soc.* 130:3296.
- Hsu FC, et al. (2008) Superconductivity in the PbO-type structure  $\alpha$ - $\text{FeSe}$ . *Proc. Natl. Acad. Sci. U.S.A.* 105:14262.
- Okabe H, Takeshita N, Horigane K, Muranaka T, Akimitsu J (2010) Pressure-induced high- $T_c$  superconducting phase in  $\text{FeSe}$ : Correlation between anion height and  $T_c$ . *Phys. Rev. B* 81:205119.
- Nabeshima F, Imai Y, Hanawa M, Tsukada I, Maeda A (2013) Enhancement of the superconducting transition temperature in  $\text{FeSe}$  epitaxial thin films by anisotropic compression. *Appl. Phys. Lett.* 103:172602.
- Wang QY, et al. (2012) Interface-induced high-temperature superconductivity in single unit-cell  $\text{FeSe}$  films on  $\text{SrTiO}_3$ . *Chin. Phys. Lett.* 29:37402.
- He S, et al. (2013) Phase diagram and electronic indication of high-temperature superconductivity at 65 K in single-layer  $\text{FeSe}$  films. *Nat. Mater.* 12:605.
- Fang MH, et al. (2008) Superconductivity close to magnetic instability in  $\text{Fe}(\text{Se}_{1-x}\text{Te}_x)_{0.82}$ . *Phys. Rev. B* 78:224503.
- Bellingeri E, et al. (2010)  $T_c = 21$  K in epitaxial  $\text{FeSe}_{0.5}\text{Te}_{0.5}$  thin films with biaxial compressive strain. *Appl. Phys. Lett.* 96:102512.
- Tsukada I, et al. (2011) Epitaxial growth of  $\text{FeSe}_{0.5}\text{Te}_{0.5}$  thin films on  $\text{CaF}_2$  substrates with high critical current density. *Appl. Phys. Express* 4:053101.
- Iida K, et al. (2011) Generic Fe buffer layers for Fe-based superconductors: Epitaxial  $\text{FeSe}_{1-x}\text{Te}_x$  thin films. *Appl. Phys. Lett.* 99:202503.
- Si W, et al. (2013) High current superconductivity in  $\text{FeSe}_{0.5}\text{Te}_{0.5}$ -coated conductors at 30 tesla. *Nat. Commun.* 4:1347.
- Zhuang JC, et al. (2014) Enhancement of transition temperature in  $\text{Fe}_x\text{Se}_{0.5}\text{Te}_{0.5}$  film via iron vacancies. *Applied Physics Letters* 104:262601.
- Wu MK, et al. (2009) The development of the superconducting PbO-type  $\beta$ - $\text{FeSe}$  and related compounds. *Physica C* 469:340.
- Maeda A, et al. (2014) Synthesis, characterization, hall effect and THz conductivity of epitaxial thin films of Fe chalcogenide superconductors. *Appl. Sur. Sci.* 312:43.
- Ichinose A, et al. (2013) Microscopic analysis of the chemical reaction between  $\text{Fe}(\text{Te},\text{Se})$  thin films and underlying  $\text{CaF}_2$ . *Supercond. Sci. Technol.* 26:075002.
- Werthamer NR, Helfand E, Hohenberg PC (1966) Temperature and purity dependence of the superconducting critical field,  $H_{c2}$ . iii. electron spin and spin-orbit effects. *Phys. Rev.* 147:295–302.
- Noji T, et al. (2010) Growth, annealing effects on superconducting and magnetic properties, and anisotropy of  $\text{FeSe}_{1-x}\text{Te}_x$  ( $0.5 \leq x \leq 1$ ) single crystals. *J. Phys. Soc. Jpn.* 79:084711.
- Lee CH, et al. (2008) Effect of structural parameters on superconductivity in fluorine-free  $\text{LnFeAsO}_{1-y}$  ( $\text{Ln} = \text{La}, \text{Nd}$ ). *J. Phys. Soc. Jpn.* 77:083704.
- Lee CH, et al. (2012) Relationship between crystal structure and superconductivity in iron-based superconductors. *Solid State Commun.* 152:644.
- Mizuguchi Y, et al. (2010) Anion height dependence of  $T_c$  for the Fe-based superconductor. *Supercond. Sci. Technol.* 23:054013.
- McQueen TM, et al. (2009) Tetragonal-to-orthorhombic structural phase transition at 90 K in the superconductor  $\text{Fe}_{1.01}\text{Se}$ . *Phys. Rev. Lett.* 103:057002.
- Horigane K, Hiraka H, Ohoyama K (2009) Relationship between structure and superconductivity in  $\text{FeSe}_{1-x}\text{Te}_x$ . *J. Phys. Soc. Jpn.* 78:074718.
- Li S, et al. (2009) First-order magnetic and structural phase transitions in  $\text{Fe}_{1+y}\text{Se}_x\text{Te}_{1-x}$ . *Phys. Rev. B* 79:054503.
- Gresty NC, et al. (2009) Structural phase transitions and superconductivity in  $\text{Fe}_{1+\delta}\text{Se}_{0.57}\text{Te}_{0.43}$  at ambient and elevated pressures. *J. Am. Chem. Soc.* 131:16944.
- Ying TP, et al. (2012) Observation of superconductivity at 30-46 K in  $\text{A}_x\text{Fe}_2\text{Se}_2$  ( $\text{A} = \text{Li}, \text{Na}, \text{Ba}, \text{Sr}, \text{Ca}, \text{Yb}, \text{and Eu}$ ). *Sci. Rep.* 2:426.
- Hatakeda T, Noji T, Kawamata T, Kato M, Koike Y (2013) New Li-ethylenediamine-intercalated superconductor  $\text{Li}_x(\text{C}_2\text{H}_5\text{N}_2)_y\text{Fe}_{2-z}\text{Se}_2$  with  $T_c = 45$  K. *J. Phys. Soc. Jpn.* 82:123705.
- Imai Y, et al. (2010) Superconductivity of  $\text{FeSe}_{0.5}\text{Te}_{0.5}$  thin films grown by pulsed laser deposition. *Jpn. J. Appl. Phys.* 49:023101.
- Imai Y, et al. (2010) Systematic comparison of eight substrates in the growth of  $\text{FeSe}_{0.5}\text{Te}_{0.5}$  superconducting thin films. *Appl. Phys. Express* 3:043102.